ORIGINAL ARTICLE

AASLD
AMERICAN ASSOCIATION FOR
THE STUDY OF LIVER DISEASES

Hepatitis E virus RNA-dependent RNA polymerase is involved in RNA replication and infectious particle production

Noémie Oechslin[1] | Nathalie Da Silva[1] | Dagmara Szkolnicka[1] | François-Xavier Cantrelle[2,3] | Xavier Hanoulle[2,3] | Darius Moradpour[1] (iD) | Jérôme Gouttenoire[1] (iD)

[1]Division of Gastroenterology and Hepatology, Lausanne University Hospital and University of Lausanne, Lausanne, Switzerland

[2]UMR1167, University of Lille, INSERM, Lille University Hospital, Institut Pasteur de Lille, Lille, France

[3]CNRS, ERL9002 - Integrative Structural Biology, Lille, France

Correspondence
Darius Moradpour and Jérôme Gouttenoire, Division of Gastroenterology and Hepatology, Centre Hospitalier Universitaire Vaudois, Rue du Bugnon 48, CH-1011 Lausanne, Switzerland.
Email: Darius.Moradpour@chuv.ch and Jerome.Gouttenoire@chuv.ch

Abstract

Background and Aims: Hepatitis E virus (HEV) is one of the most common causes of acute hepatitis worldwide. Its positive-strand RNA genome encodes three open reading frames (ORF). ORF1 is translated into a large protein composed of multiple domains and is known as the viral replicase. The RNA-dependent RNA polymerase (RDRP) domain is responsible for the synthesis of viral RNA.

Approach and Results: Here, we identified a highly conserved α-helix located in the RDRP thumb subdomain. Nuclear magnetic resonance demonstrated an amphipathic α-helix extending from amino acids 1628 to 1644 of the ORF1 protein. Functional analyses revealed a dual role of this helix in HEV RNA replication and virus production, including assembly and release. Mutations on the hydrophobic side of the amphipathic α-helix impaired RNA replication and resulted in the selection of a second-site compensatory change in the RDRP palm subdomain. Other mutations enhanced RNA replication but impaired virus assembly and/or release.

Conclusions: Structure-function analyses identified a conserved amphipathic α-helix in the thumb subdomain of the HEV RDRP with a dual role in viral RNA replication and infectious particle production. This study provides structural insights into a key segment of the ORF1 protein and describes the successful use of reverse genetics in HEV, revealing functional interactions between the RDRP thumb and palm subdomains. On a broader scale, it demonstrates that the HEV replicase, similar to those of other positive-strand RNA viruses, is also involved in virus production.

Abbreviations: aa, amino acid; gt, genotype; ORF, open reading frame; NMR, nuclear magnetic resonance; RDRP, RNA-dependent RNA polymerase.

Noémie Oechslin and Nathalie Da Silva contributed equally to the study.

This article is dedicated to the memory of Stefan Kunz, a wonderful scientist and friend, whose passion for virology inspired many.

- -

INTRODUCTION

HEV is a positive-strand RNA virus classified in the *Hepeviridae* family.[1] Members of this family infect diverse hosts, including, among others, fish, birds, bats, ferrets, moose, pigs, and humans. Most human pathogenic strains belong to species *Orthohepevirus A*. HEV genotypes (gt) 1 and 2 are transmitted from humans to humans by the fecal-oral route and can cause large waterborne outbreaks in resource-limited settings.[2] HEV gt 3 and 4 represent a primarily porcine zoonosis and are transmitted by the consumption of undercooked meat products in resource-rich settings as well. Hence, HEV infection represents a major cause of acute hepatitis and a growing global health concern worldwide.[3–5] HEV gt 3 can trigger acute-on-chronic liver failure in patients with preexisting cirrhosis, cause neurologic as well as other extrahepatic manifestations, and persist in individuals who are immunocompromised, leading to chronic hepatitis with potential rapid evolution to cirrhosis.[6]

HEV has a 7.2-kb positive-strand RNA genome encoding three open reading frames (ORF), which are translated into (1) the ORF1 protein representing the viral replicase, (2) the ORF2 protein corresponding to the capsid, and (3) ORF3, a small, palmitoylated protein involved in virion secretion.[7–9] The ORF1 protein is composed of multiple domains that have been defined primarily on the basis of sequence homology with other viruses. Whether these domains are processed into individual proteins or act as one large polyprotein is still a matter of debate.[7,9] Although the functions of the Y domain, the putative papain-like cysteine protease, and the hypervariable region are uncertain, other domains have a defined function, including a methyltransferase, a macro domain, an RNA helicase, and an RNA-dependent RNA polymerase (RDRP).[10] The RDRP catalyzes the synthesis of viral RNA, including the full-length and subgenomic positive-strand RNAs as well as the negative-strand RNA, which serves as a template for positive-strand RNA synthesis.

The HEV RDRP has been poorly studied thus far. Polymerase activity of recombinant RDRP in vitro and a high affinity of this domain for the 3′ noncoding region of the genome have been demonstrated.[11] Based on the high conservation of this enzyme throughout all virus families, it is expected that it adopts a closed "right hand" three-dimensional organization with three distinct subdomains, namely the palm, thumb, and fingers. Conserved motifs involved in the catalytic activity of RDRPs, referred to as A to D, reside in the central palm subdomain constituting the enzymatic core region of the polymerase. These motifs have been partially mapped for the HEV RDRP by homology-based analyses.[10,12] Interestingly, a mutation in the RDRP identified in patients with chronic hepatitis E and ribavirin treatment failure, i.e., G1634R, displays significantly increased polymerase activity.[13,14] Therefore, a recent study took advantage of this variant to establish a robust HEV cell culture system.[15]

In the present study, we report the three-dimensional structure of a conserved amphipathic α-helix in the thumb subdomain of the HEV RDRP. Site-directed mutagenesis targeting the conserved residues and functional analyses revealed a dual role of this structural element in HEV RNA replication and virus production. Moreover, taking advantage of a selectable subgenomic replicon, we could identify a compensatory second-site change in the palm subdomain of the RDRP, revealing a functional interaction between the α-helix in the thumb and a predicted α-helix in the palm subdomains. By homology modeling with RDRPs of other positive-strand RNA viruses, our findings suggest that the amphipathic α-helix identified in the thumb subdomain is very close to the predicted first α-helix of the palm subdomain and that it may regulate the activity of the HEV RDRP in RNA replication and virus production.

MATERIALS AND METHODS

Cell lines

S10-3 human hepatocellular carcinoma cells (kindly provided by Suzanne U. Emerson, National Institutes of Health, Bethesda, MD) and HepG2/C3A hepatoblastoma cells (American Type Culture Collection CRL-10741) were maintained in Dulbecco's modified Eagle's medium supplemented with 10% fetal bovine serum.

Plasmids, in vitro transcription, and RNA transfection

All constructs prepared in this study as well as in vitro transcription and RNA transfection are described in the Supporting Information.

Nuclear magnetic resonance structural analyses

The nuclear magnetic resonance (NMR) structural analyses are described in the Supporting Information.

Virus infection and determination of infectivity

Five days after transfection with in vitro transcribed full-length HEV RNA, culture supernatants and S10-3 cells were harvested to determine infectivity in the extracellular and intracellular compartments, respectively. Cell pellets were subjected to 3 freeze-and-thaw cycles, followed by centrifugation for 15 min at 3000× *g* to prepare

the intracellular sample. Infectivity was determined in duplicate by focus formation assay after inoculation of HepG2/C3A cells seeded into a 24-well plate with 1/10 of the total extracellular (200 µl) or intracellular (50 µl) virus sample and culture in Eagle's minimum essential medium supplemented with 2% low-IgG fetal bovine serum.[15] Cells were fixed 5 days postinoculation and stained using an anti-ORF2 rabbit polyclonal antibody kindly provided by Rainer G. Ulrich (Friedrich Loeffler Institute, Greifswald, Germany).

Luciferase assays

Gaussia luciferase activity was measured in culture supernatants from cells transfected with HEV83-2_Gluc–derived constructs. Culture medium was collected daily and stored at −20°C until measurement. Luciferase activity was measured in duplicate after the addition of 60 µl coelenterazine substrate (0.8 µM) to 10 µl of culture medium for 5 s using a Berthold luminometer (Bad Wildbad, Germany).

Statistical analyses

Significance values were calculated by using the unpaired t test with the GraphPad Prism 6 software package (GraphPad Software).

Data availability

All relevant data are within the paper and its Supporting Information files. Raw data are available in Zenodo repository (https://doi.org/10.5281/zenodo.4541208).

RESULTS

The thumb subdomain of the HEV RDRP comprises a conserved predicted α-helix

Alignment of the RDRP sequences from phylogenetically distant *Hepeviridae* family members, i.e., HEV gt 1 and 3 as well as avian, ferret, bat, moose, and trout HEV (Figure S1), combined with secondary structure predictions revealed a high degree of structural conservation (Figure S2), especially of palm subdomain motifs A-D where amino acid (aa) sequences are also highly conserved (Figure 1). Alignment of the RDRP sequences from HEV gt 3 (83-2-27 strain; aa 1115–1703) and other positive-strand RNA viruses for which a polymerase structure has been solved, e.g., Norwalk virus (*Caliciviridae* family; *Norovirus* genus; Ast6139/01/Sp strain) (Figure S3), confirms the positions of motifs A-D with respect to the secondary structure prediction in the palm subdomain.[16] The C-terminal region of the HEV RDRP, corresponding to the thumb subdomain,

is predicted to display a structure different from that of other positive-strand viruses (Figure S3) but appears to be conserved within the *Hepeviridae* family but with an aa sequence identity of only 30%–50% (Figures 1 and S2). Within the thumb subdomain, aa segment 1630–1645 shows a strong and conserved prediction for an α-helical fold in all *Hepeviridae* family members despite relatively low aa sequence conservation. Interestingly, Gly 1634, which has been found to be substituted by arginine in patients with chronic hepatitis E and ribavirin treatment failure (G1634R variant), is located at the end of this segment.

NMR structure of ORF1 protein segment 1622–1647 reveals an amphipathic α-helix

Conservation of an α-helix prediction throughout the *Hepeviridae* family and the location of variant G1634R prompted us to solve the structure of ORF1 protein segment 1622–1647 by NMR. Tested in different conditions, a ^{15}N and ^{13}C doubly labeled recombinant ORF1[1622–1647] peptide produced in *Escherichia coli* yielded well-resolved NMR spectra in the presence of 20% trifluoroethanol (TFE), allowing determination of its three-dimensional structure (Figures S4 and S5). ^{13}C secondary NMR chemical shifts (dCA-dCB) obtained for ORF1[1622–1647], with dCA and dCB corresponding to the difference between the experimental and the random coil chemical shift values for [13]Cα and [13]Cβ, respectively, served to determine the secondary structure propensity of the peptide at each position (Figure 2A,B). The latter analysis clearly revealed an α-helical fold of the peptide spanning from Pro 1628 to Gly 1644 (Figure 2B). The 20 best conformers obtained showed a regular α-helical conformation extending from residues 1628 to 1644, as revealed by the nearly perfect backbone superimposition within this region (Figure 2C). The per-residue backbone root-mean-square deviation values showed that the extremities of the peptide are, however, highly flexible (Figure 2D). As illustrated in Figure 2E for the representative structure of ORF1[1622–1647], the central part of the helix including residues Pro 1628 to Gly 1644 clearly exhibits an amphipathic character with most hydrophobic as well as neutral residues exposed on one side (upper part of the panel) and charged as well as polar residues on the opposite side of the helix (lower part). This amphipathic character is further supported by the observed behaviors of the peptide in aqueous buffer and in the presence of TFE.

The conserved hydrophobic face of ORF1 protein α-helix 1628–1644 is involved in HEV RNA replication

In order to characterize the functional role of amphipathic α-helix 1628–1644, a panel of mutations targeting the strictly conserved residues was prepared in a
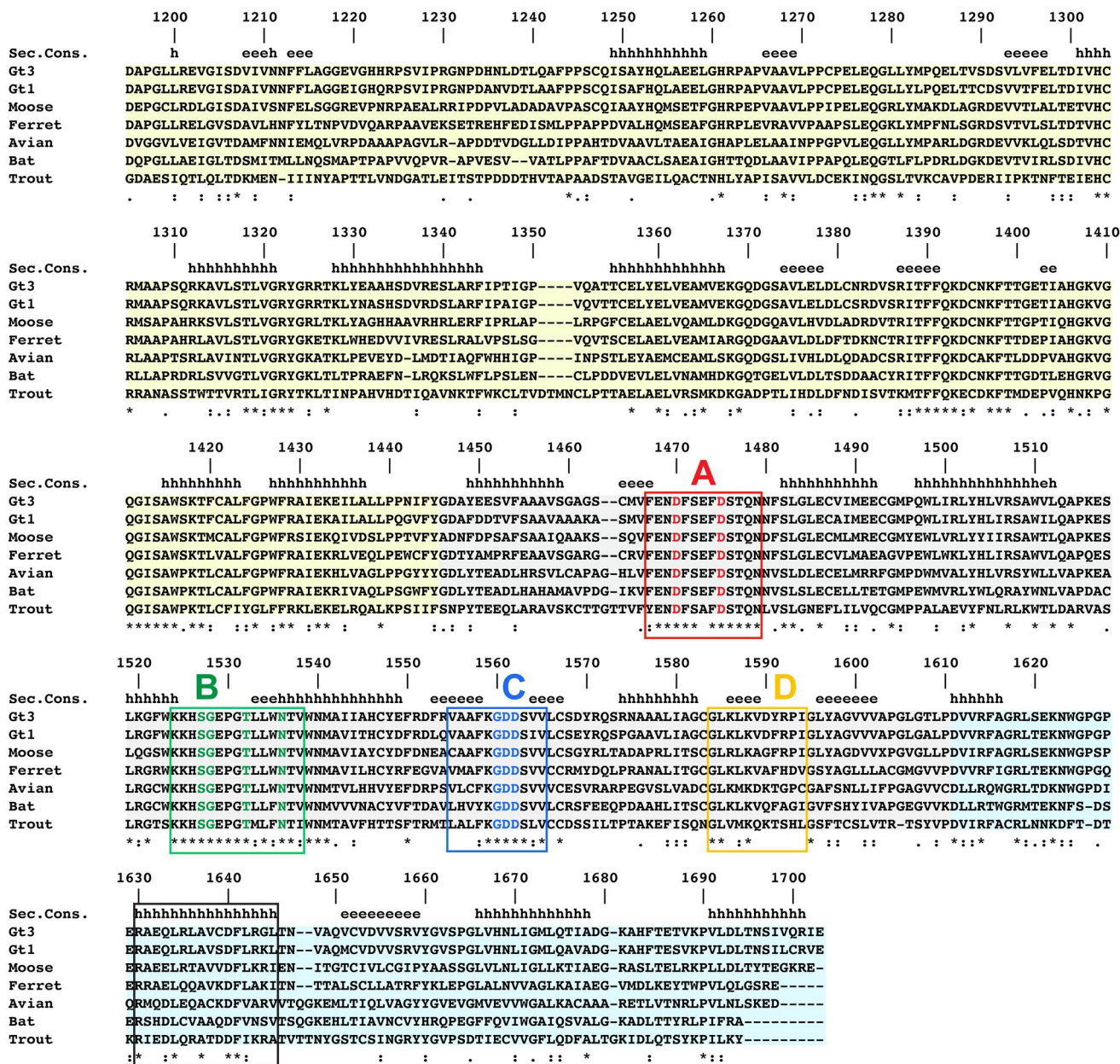
FIGURE 1 A conserved α-helix is predicted in the thumb subdomain of the HEV RDRP. Sequence analysis of the RDRP domain of the HEV ORF1 protein. aa sequence alignment of the RDRP domains from a broad range of *Hepeviridae* family members (see details in Figure S2). A consensus secondary structure prediction (Sec. Cons.) for all sequences was determined on the basis of the algorithms DSC, GOR IV, HNN SIMPA96, PREDATOR, SOPM, and PHD available at https://npsa-prabi.ibcp.fr, as shown above the alignment (h, α-helix; e, extended strand). Random coil or discrepant predictions are not indicated. The degree of aa physicochemical conservation at each position is shown on the bottom line and can be inferred from the similarity index according to ClustalW convention (asterisk, invariant; colon, highly similar; dot, similar). The fingers, palm, and thumb subdomains are denoted by light yellow, gray, and blue backgrounds, respectively. The conserved RDRP motifs A–D in the palm subdomain are indicated by colored boxes, and the fully conserved residues are highlighted in the same color. The predicted α-helix in the thumb subdomain is highlighted by a black square. Numbering of aa is relative to the ORF1 protein sequence from HEV gt 3 strain 83-2-27 (AB740232) [Color figure can be viewed at wileyonlinelibrary.com]

gt 3 subgenomic replicon allowing the expression of Gaussia luciferase[17] (Figure 3). Conserved residues were substituted by alanine, which should preserve the α-helical fold, with the exception of Ala 1637, which was substituted by a leucine (Mut A_L), a larger and hydrophobic residue that satisfies the physicochemical properties of this face of the α-helix.

Alanine substitution of Leu 1634 (Mut L_A) or Phe 1641 (Mut F_A) or disruption of the amphipathic character of α-helix 1628–1644 by insertion of an alanine between Leu 1634 and Arg 1635 (Ins +1A) strongly impaired HEV RNA replication, as shown by luciferase values comparable with those of the replication-deficient control GAD (Figure 3A). Substitution of Arg 1630 by
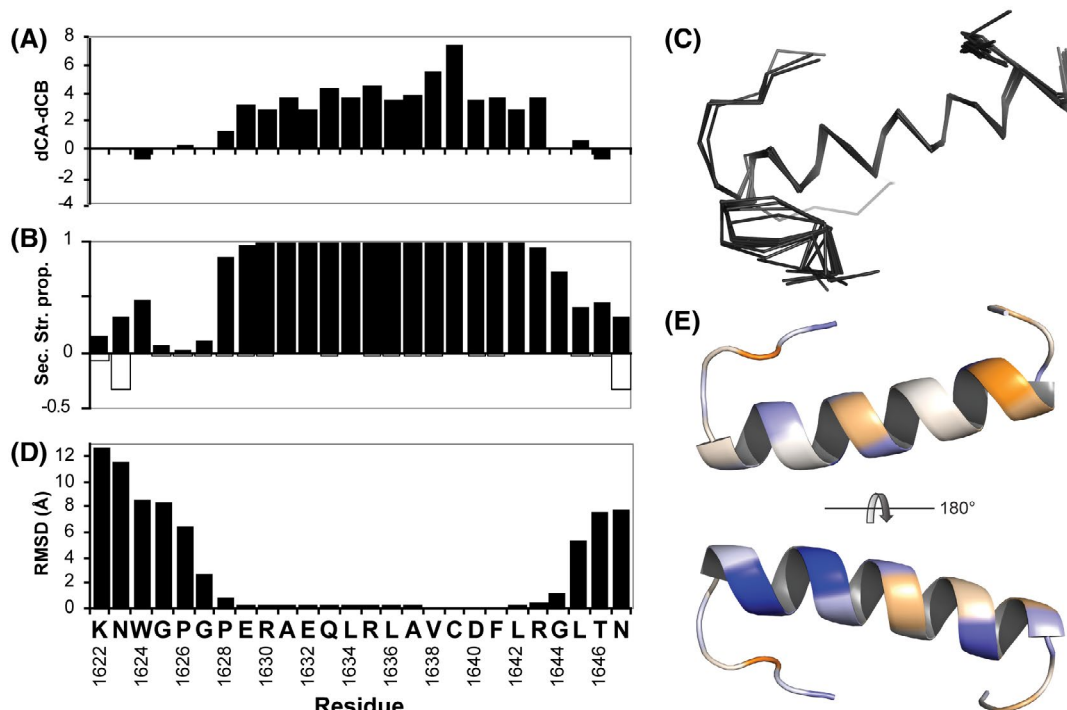
FIGURE 2 ORF1 protein aa 1628–1644 fold into an amphipathic α-helix. (A) ^{13}C secondary NMR chemical shifts of ORF1[1622–1647]. The secondary NMR chemical shifts (dCA-dCB) are shown along the peptide sequence corresponding to ORF1 protein aa 1622–1647, with dCA and dCB corresponding to the difference between the experimental and the random coil chemical shift values for [13]Cα and [13]Cβ, respectively. Positive and negative values indicate the presence of α-helix and β-sheet, respectively. (B) Secondary structure propensity for ORF1[1622–1647]. Positive (black bars) and negative (white bars) values correspond to α-helix and β-sheet, respectively. (C) Superimposition of the 20 lowest energy conformers (Cα traces) of ORF1[1622–1647] that have been generated by CS-Rosetta using ^{1}H and ^{13}C NMR chemical shifts. (D) Local root-mean-square deviation (RMSD) values (Å) for the backbone atoms (N, Cα, and C') of each residue in the final bundle of structures in (C). (E) The amphipathic feature of the α-helix in ORF1[1622–1647] is highlighted on the lowest energy structure, which is colored according to the Wimley and White hydrophobicity scale[33] ranging from hydrophilic (blue) to hydrophobic (orange) [Color figure can be viewed at wileyonlinelibrary.com]

alanine and of Ala 1637 by leucine (Mut R_A and Mut A_L, respectively) decreased replication by about 30-fold. Surprisingly, alanine substitution of the conserved negatively charged residue Asp 1640 (Mut D_A) did not impair but increased replication approximately 2-fold (Figure 3A). This phenotype resembles the one of variant G1634R as described in the HEV gt 3 Kernow-C1 p6 clone[13] and confirmed here in the 83-3-27 clone (Mut G_R). To explore the importance of structural as compared with aa sequence conservation, chimeric constructs were prepared by swapping part of the HEV gt 3 1628–1644 segment with those from moose (GenBank accession number KF951328) or ferret HEV (JN998607). Interestingly, like Mut D_A and Mut G_R, the replication capacity of chimeras Chim_moose and Chim_ferret was increased as compared with the wild-type construct (Figure 3A).

Taken together, these results confirm the importance of α-helix 1628–1644 and the conserved residues on its hydrophobic face for HEV RNA replication (Figure 3B). Furthermore, they demonstrate that some mutations within this segment, especially those located on the hydrophilic face, including the

naturally occurring variant G1634R, enhance HEV RNA replication.

ORF1 protein α-helix 1628–1644 is involved in virus production

To evaluate the functional consequences on virus production of the mutations that do not impair RNA replication, full-length HEV genomes were prepared and analyzed for intracellular and extracellular infectivities. As shown in Figure 4, all of these mutations reduced virus production although they provided a replication advantage in the subgenomic replicon context (Figure 3). Indeed, total infectivity measured at day 5 posttransfection was at least 40% lower as compared with the wild type, suggesting impaired assembly of infectious virus (Figure 4). Furthermore, the ratio between intracellular and extracellular infectivities, which provides a quantitative evaluation of infectious particle release, revealed that secretion of Mut G_R and Chim_moose is reduced by about 2-fold (Figure 4). As expected, a full-length construct with a mutated ORF3 start codon
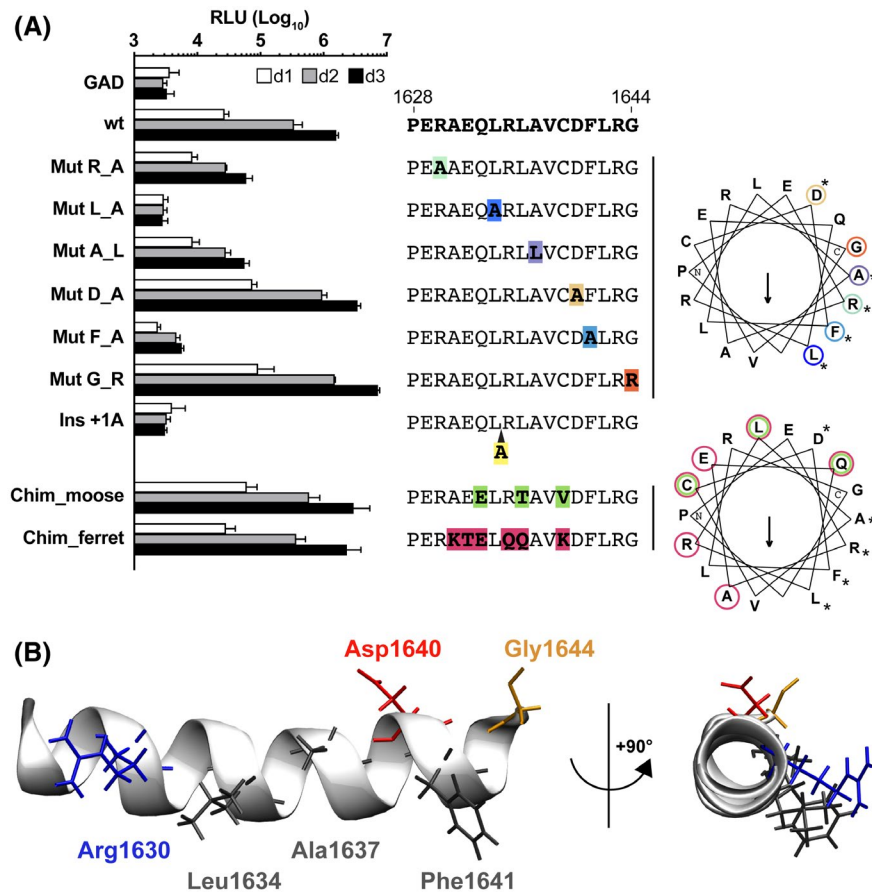
FIGURE 3 The conserved hydrophobic face of ORF1 protein α-helix 1628–1644 is involved in HEV RNA replication. (A) Replication of subgenomic HEV replicons harboring mutations in α-helix 1628–1644. S10-3 human hepatocellular carcinoma cells were transfected with subgenomic HEV replicons harboring a Gaussia luciferase reporter and the mutations indicated in the sequences and the captions. The bars indicate relative light units (RLU; mean ± SD) determined at day 1, 2, and 3 posttransfection. GAD denotes a replication-defective control replicon harboring an alanine substitution in the GDD motif of the RDRP. wt denotes the parental wild-type replicon. Helix projections drawn on the basis of the NMR structure are shown on the right, with the mutated residues circled in color. The hydrophobic moment, calculated by HeliQuest (https://heliquest.ipmc.cnrs.fr),[34] is indicated by an arrow. Asterisks denote residues that are conserved among all *Hepeviridae*. (B) Ribbon representation of the NMR structure model of ORF1 segment 1627–1644. Residues investigated in the replication assay are shown with their lateral chain and are color-coded, i.e., hydrophobic in black, polar in orange, basic in blue, and acidic residues in red. The α-helix is shown with the hydrophobic side beneath and hydrophilic side on top and presented either from the side (left) or in profile (right) [Color figure can be viewed at wileyonlinelibrary.com]

(ΔORF3) did not show any infectious particle secretion.[8] Interestingly, we observed that infection with Mut G_R yielded larger foci than the other mutants, indicating more efficient cell-to-cell spread (Figure S6).

Taken together, these results demonstrate that the ORF1 protein, i.e., the viral replicase and, more specifically, the RDRP domain, is involved in virus production, including the assembly as well as the release of infectious particles.

Reverse genetics indicate a functional interaction between the HEV RDRP thumb and palm subdomains

Mutations Mut R_A, Mut L_A, Mut A_L and Mut F_A, which impaired HEV RNA replication, were introduced into a subgenomic replicon harboring a neomycin resistance cassette[17] in order to select second-site compensatory changes (Figure 5A). Although Mut L_A and Mut F_A did not yield any G418-resistant cells, Mut A_L and Mut R_A allowed the selection of G418-resistant clones after 13 days of antibiotic treatment. Crystal violet staining showed a reduced efficiency of colony formation of Mut R_A as compared with the wild type (7.4×10^4 versus 2.5×10^5 clones per microgram RNA, respectively) (Figure 5B), in line with the results from transient replication assays (Figure 3A). Sequencing of the region corresponding to RDRP aa 1370–1703 from the G418-resistant cell population revealed the retention of Mut R_A and the appearance of a Glu-to-Lys substitution in the first predicted α-helix of the palm subdomain preceding motif A (E1451K; see Figure 1). No compensatory change was identified for Mut A_L.
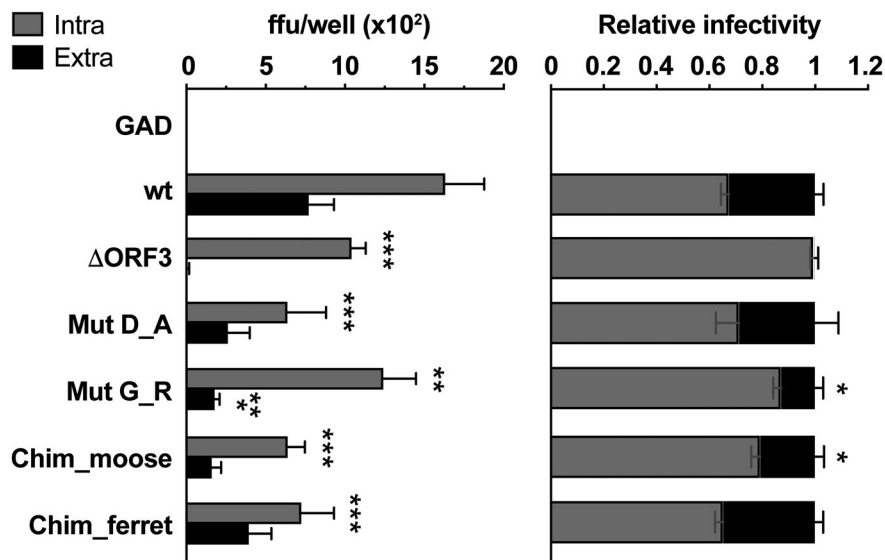
FIGURE 4 ORF1 protein α-helix 1628–1644 is involved in virus production. S10-3 human hepatocellular carcinoma cells were transfected with full-length HEV RNA harboring replication-competent mutations Mut D_A, Mut G_R, Chim_moose, and Chim_ferret (see Figure 3). A parental wild-type (wt) and a replication-defective (GAD) genome served as positive and negative controls, respectively. ΔORF3 denotes a full-length HEV RNA that does not produce ORF3 protein. Total intracellular and extracellular infectivities were determined at day 5 posttransfection by focus formation assay. The bars indicate focus forming units (ffu; mean ± SD) determined in at least two titrations of three independent experiments (left panel). The ratio of extracellular versus intracellular infectivity is represented on the right, with total infectivity normalized to 1 for each construct. Statistical differences (Mann-Whitney test) compared with wt are denoted by * and ** for $p < 0.05$ and < 0.001, respectively

To confirm the replication advantage conveyed by the E1451K substitution, subgenomic replicon constructs expressing a luciferase reporter and harboring the substitution (Palm E_K) alone or in combination with Mut R_A were prepared and assayed. As shown in Figure 5C, Mut R_A alone led to an approximately 30-fold decrease in RNA replication, which was fully compensated by the E1451K substitution (Mut R_A/ Palm E_K). An about 3-fold increase in replication capacity as compared with the wild type was observed for Palm E_K alone, which in itself does not fully compensate for the 30-fold decrease in replication observed for Mut R_A. Therefore, the E1451K substitution in the RDRP palm subdomain may be considered as a compensatory mutation in response to Mut R_A, indicating a functional interaction between the two positions in the thumb and palm subdomains.

To evaluate whether adaptive change E1451K in the palm subdomain (Palm E_K) can also restore virus production of Mut R_A, the corresponding substitutions were introduced into a full-length HEV genome and analyzed for intracellular and extracellular infectious virus production. As shown in Figure 5D, poorly replicating Mut R_A did not yield an infectious virus, whereas Palm E_K showed a 2-fold decrease of total infectivity as compared with the wild type. Interestingly, the combination of these mutations (Mut R_A/Palm E_K), known to replicate as the wild type (Figure 5C), showed only a very poor capacity to produce an infectious virus. These findings further confirm the importance of conserved α-helix 1628–1644 in the RDRP thumb subdomain for HEV production.

Conserved α-helix 1628–1644 in the RDRP thumb subdomain is an important structural element regulating HEV RNA replication and virus production

The thumb subdomain is known to be the RDRP region with the highest structural variability among viruses.[18] However, RDRPs show an overall three-dimensional organization that is very similar between viruses, with interactions between the fingers and thumb subdomains that completely encircle the active site of the enzyme and contribute to the formation of a channel where the nucleic acid is synthesized on the basis of its template. Hence, in respect to known RDRP structures, notably the one from Norwalk virus that we used as template in this study, we can predict that amphipathic α-helix 1628–1644 in the thumb subdomain is located closely to the first α-helix of the palm subdomain in which the E1451K compensatory change resides (Figure 6). The contribution of the conserved residues of this α-helix to RNA replication as well as its amphipathic character suggest that the hydrophobic side of the α-helix is oriented toward the core structure of the enzyme. This implies that the less conserved hydrophilic side may be surface-exposed, with residue Asp 1640, involved in virus assembly, being potentially engaged in interactions with other partners.
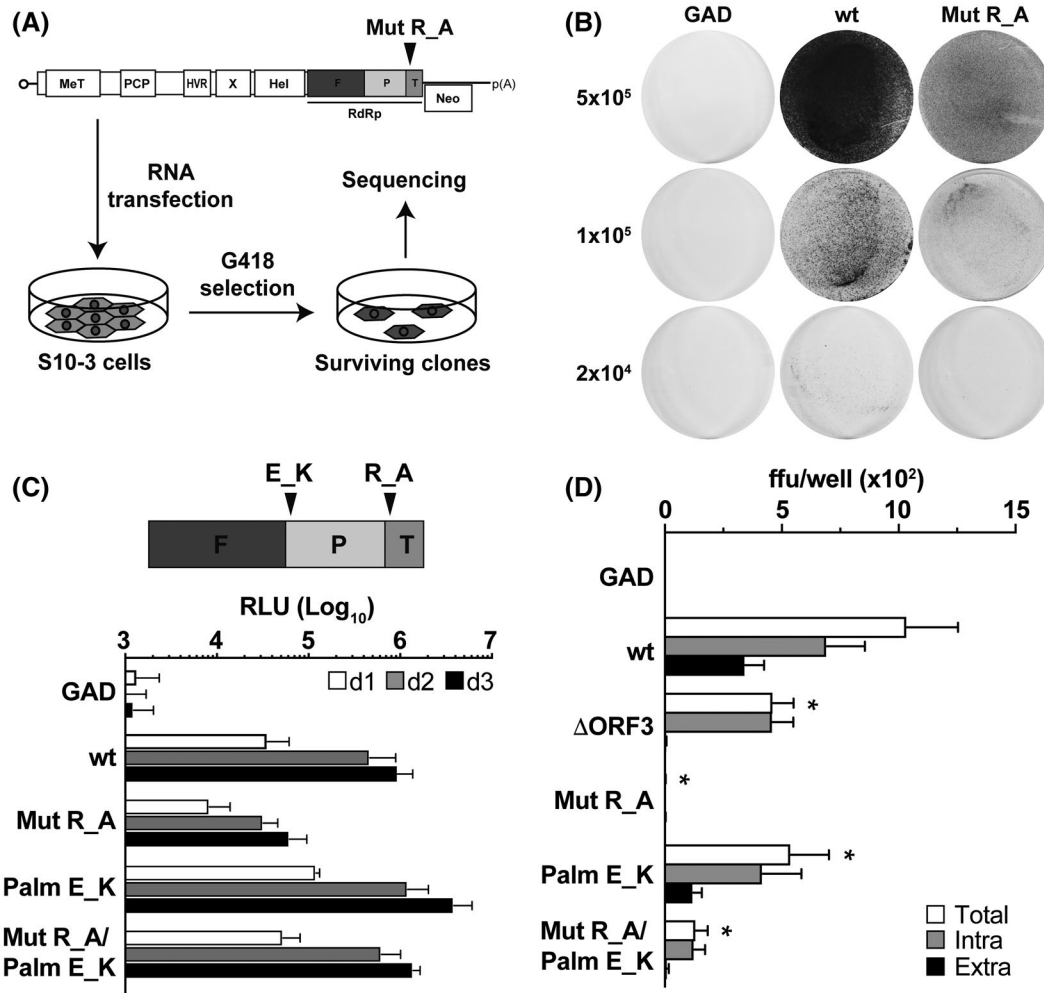
FIGURE 5 Reverse genetics indicate a functional interaction between the HEV RDRP thumb and palm subdomains. (A) Schematic representation of the subgenomic HEV replicon used to select for second-site adaptive changes. In vitro–transcribed replicon RNA was electroporated into S10-3 cells and maintained under selection with 500 µg/ml G418 for at least 13 days. The selected G418-resistant cells were then lysed for total RNA extraction, and sequence analysis was performed to identify potential adaptive changes in the RDRP sequence. (B) Selection of G418-resistant cells replicating the HEV Mut R_A replicon. S10-3 cells were electroporated with Mut R_A replicon RNA or GAD or wild-type (wt) parental replicon RNAs as negative and positive controls, respectively, followed by G418 selection for 10 days and crystal violet staining. The number of electroporated cells plated in a 100-mm dish is indicated on the left. Results of a representative experiment are shown. (C) Replication of subgenomic HEV replicons harboring mutations in α-helix 1628–1644. S10-3 cells were transfected with subgenomic HEV replicons harboring a Gaussia luciferase reporter and single mutations Mut R_A or Palm E_K or the double mutation Mut R_A/Palm E_K. The bars indicate relative light units (RLU; mean ± SD) determined at day 1, 2, and 3 posttransfection. A scheme representing the RDRP fingers (F), palm (P), and thumb (T) subdomains is shown to denote the position of Mut R_A and the Palm E_K change (arrowheads). (D) Infectious virus production by HEV genomes harboring Mut R_A and the Palm E_K change. S10-3 cells were transfected with HEV full-length RNA constructs harboring single mutations Mut R_A or Palm E_K or the double mutation Mut R_A/Palm E_K. Wild-type (wt), replication-defective (GAD), and ORF3-deficient (ΔORF3) genomes served as positive, negative, and secretion-deficient controls, respectively. Total intracellular and extracellular infectivities were determined at day 5 posttransfection by focus formation assay. The bars indicate focus forming units (ffu; mean ± SD) determined in at least two titrations of three independent experiments. Statistical differences (Mann-Whitney test) for total infectivity as compared with wt are denoted by an asterisk for $p \leq 0.0001$

DISCUSSION

In the present study, we structurally and functionally characterized a conserved amphipathic α-helix in the C-terminal region of HEV ORF1 protein, more precisely in the thumb subdomain of the RDRP. NMR analyses revealed an amphipathic α-helix extending from aa 1628 to 1644. Conserved residues on the hydrophobic side of this helix were found to be essential for RNA replication, whereas residues on the hydrophilic side were found to be involved in infectious particle production. Reverse genetics allowed for identification of a functional interaction and likely close proximity between the amphipathic α-helix in the thumb subdomain and a predicted α-helix in the palm subdomain.

Structural information for HEV, and in particular for the ORF1 protein, is very limited. A recent crystal structure of the putative papain-like cysteine protease
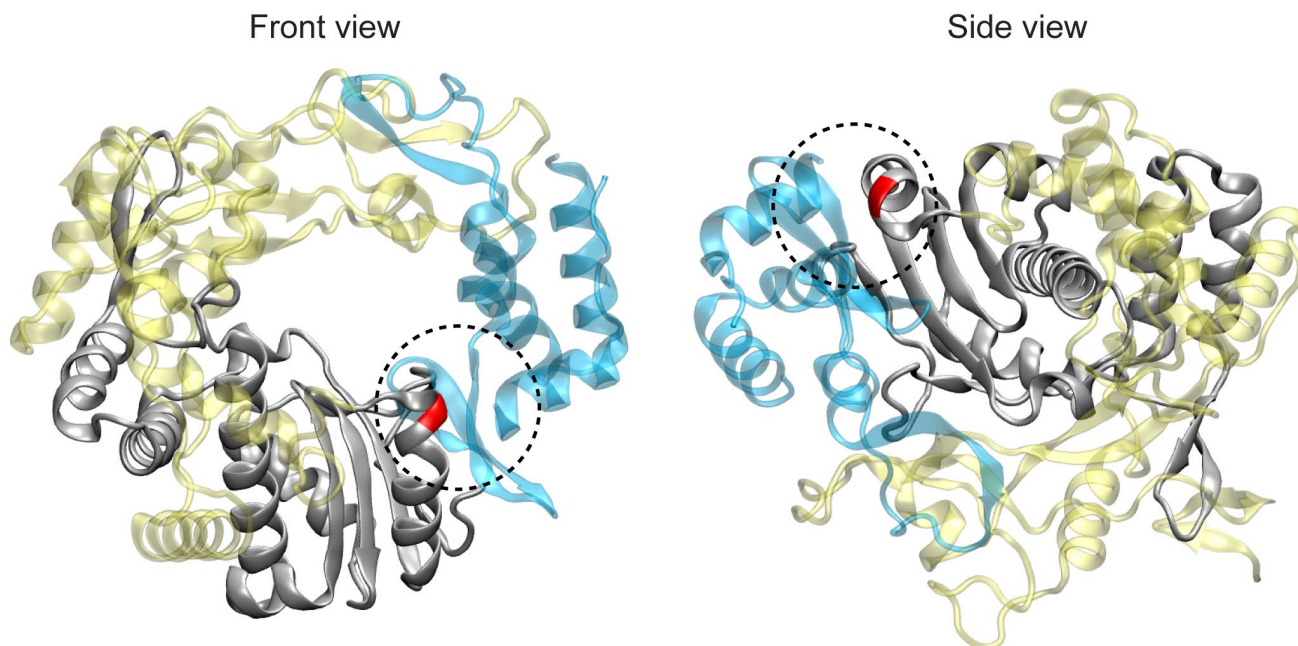
Front view   Side view

FIGURE 6   The amphipathic α-helix of the RDRP thumb subdomain is located in close proximity to the first α-helix of the palm subdomain. RDRP crystal structure model (3BSN) of Norwalk virus strain Ast6139/01/Sp bound to primer-template RNA.[35] Fingers, palm, and thumb subdomains are shown in yellow, gray, and cyan, respectively. The position of the compensatory change identified in the HEV RDRP palm subdomain is highlighted in red, and the predicted location of amphipathic α-helix 1628–1644 in the thumb subdomain is indicated by a dashed black circle [Color figure can be viewed at wileyonlinelibrary.com]

domain revealed a high structural homology to fatty acid binding domains.[19] Although an enzymatic activity of this domain has not yet been proven, the structure provides a framework for future functional studies. Amphipathic α-helix 1628–1644, described here, is only the second structurally solved segment of the ORF1 protein. Although representing a short element, structure-function analyses allowed us to identify a dual role of the HEV RDRP in RNA replication and virus production as well as a functional interaction between the thumb and palm subdomains. However, a complete structure of the HEV RDRP domain will be required to map the determinants of enzymatic activity and other functions as well as to design direct antiviral agents.

Viral evolution can serve to identify mutations that favor virus fitness. Reverse genetics, allowing the identification of second-site compensatory changes, have been applied to the study of diverse positive-strand viruses, e.g., alpha-, flavi-, or picornaviruses.[20–22] Among them, a remarkable example is HCV and the opportunities offered by the development of a selectable subgenomic replicon system.[23,24] This system enabled rapid advances in the understanding of the virus life cycle by the identification of cell culture adaptive changes as well as the mapping of functional links between viral proteins, including between structural and nonstructural proteins.[25] In addition, it allowed for the identification of nonstructural protein 5A inhibitors as potent antivirals for the treatment of hepatitis C.[26]

Here, we applied reverse genetics to the study of HEV. Using a selectable subgenomic replicon, we identified a compensatory mutation in the RDRP palm subdomain (Palm E_K) in response to a mutation introduced in the α-helix in the thumb subdomain (Mut R_A), indicating a functional and likely structural interaction. Future studies may benefit from this approach.

Strikingly, substitution of a conserved positively charged residue, i.e., Arg at position 1630 (Mut R_A), led to the appearance of a positively charged residue, i.e., Lys at position 1451, which likely compensates for the loss of positive charge. Given the predicted close proximity of the two α-helices in the three-dimensional structure of the RDRP (Figure 6), it is plausible that electrostatic interactions between these segments stabilize the conformation of the polymerase to maintain efficient catalytic activity.

Interestingly, the identified α-helix in the thumb subdomain has an amphipathic character. Amphipathic helices are usually engaged in hydrophobic interactions with other elements, e.g., cellular membranes or proteins. As we did not observe any interaction of the ORF1 protein aa 1622 to 1647 segment or of the entire RDRP domain with cellular membranes (data not shown), we hypothesize that the hydrophobic side of the α-helix faces the core of the enzyme, i.e., the palm subdomain, whereas the hydrophilic side may be surface-exposed. This implies that the absolutely conserved residues involved in RNA replication and

located on the hydrophobic side of the α-helix, i.e., Arg 1630, Leu 1634, Ala 1637, and Phe 1641, interact with the palm subdomain, the most conserved region of the RDRP.

Based on these observations, Asp 1640, which is located on the hydrophilic side and involved in virus production, would be surface-exposed. Conservation of α-helix 1628–1644 and residue Asp 1640 throughout all *Hepeviridae* family members points toward a shared molecular mechanism connecting RNA synthesis and virus assembly. Residue Asp 1640 may be involved in a specific protein–protein interaction with a viral or host factor to favor RNA encapsidation. The *Hepeviridae* represent a family of viruses with a broad host range infecting diverse animal species. Hence, interaction of residue Asp 1640 with a viral factor is more likely as compared with a host factor, which would have to be conserved from fish or birds to humans. Contribution of the HEV RDRP, and especially of α-helix 1628–1644 in the thumb subdomain, to virus assembly may, therefore, be mediated through interaction with a viral factor such as the ORF2 protein. Indeed, the capsid protein is highly conserved, especially in its central region, and a plausible interaction partner of the RDRP in viral RNA encapsidation.

The thumb subdomain of the RDRP from other viruses, including poliovirus,[27] is essential for multimerization of the polymerase. It is also plausible, therefore, that the oligomerization state of the enzyme determines its contribution to virus production. The replication machineries of an increasing number of viruses have been shown to be involved in virus assembly.[28] For example, nonstructural protein 5A, an essential component of the HCV replicase, is believed to contribute to virus assembly by transferring newly synthesized RNA genomes to the viral capsid (reviewed in Lindenbach and Rice[29]). Moreover, cell culture adaptation of an HCV infectious clone led to selection of two changes in the viroporin p7 and the fingers subdomain of the RDRP NS5B, which greatly enhanced specific infectivity, revealing a direct role of the polymerase in virus assembly.[30]

Taken together, the functional data collected in this study demonstrate that mutations in α-helix 1628–1644 increasing RNA replication affect virus production (Figure S7). HEV has to keep an equilibrium between RNA replication and virus production. Our observations, therefore, raise the possibility that the HEV RDRP regulates the balance between RNA replication and virus production to maintain efficient viral propagation. Furthermore, our results indicate that the HEV polymerase activity has the potential to be enhanced by genetic changes. Supporting this hypothesis, several naturally occurring mutations have been found to enhance RNA replication, including insertions in the hypervariable region as well as substitutions Y1320H and G1634R in the RDRP (reviewed in Todt et al.[31]).

Surprisingly, we did not only observe an effect of mutations in the α-helix within the thumb subdomain on virus assembly but also on particle secretion (Figure 4). Two mutants that did not impair RNA replication, i.e., Mut G_R and Chim_moose, showed a 2-fold decrease in virus secretion in addition to reduced infectious virus production. Of note, Mut G_R corresponds to the G1634R variant selected in patients who are immunocompromised with chronic hepatitis E and ribavirin treatment failure. Interestingly, a positively charged residue, either Arg or Lys, is found in this position in most *Hepeviridae* family members, but a glycine is present in 80% of HEV gt 3 isolates.[13] The antiviral effect of ribavirin is mediated through depletion of the guanosine triphosphate pool[32] and its mutagenic properties.[14,31] Because HEV does not face strong immune selective pressure in patients with chronic hepatitis E, suboptimal ribavirin treatment is more likely to induce mutations of the genome that favor replication to escape drug pressure. The selection of a variant with increased RNA replication capacity, i.e., G1634R, is in line with this hypothesis.

Todt et al. recently developed a robust infection system using HEV gt 3 genomes harboring the G1634R mutation.[15] In accordance with our study, they observed an impaired secretion with significant intracellular accumulation of virus harboring the G1634R change in either the p6 or 83-2-27 infectious clones.[15] By measuring infectivity at an earlier time point (day 5 as compared with day 7 in the study by Todt et al.), we could show that the G1634R substitution can also affect virus assembly. Hence, the increase in intracellular infectivity observed by Todt et al.[15] may be a consequence of the more efficient cell-to-cell spread of the G1634R variant, as observed in their as well as in our study (Figure S6). Although these observations may have important implications for the understanding of ribavirin treatment failure, future studies will have to address the mechanism(s) by which a mutation in the RDRP domain favors cell-to-cell spread.

To conclude, our study provides structural insight into the HEV RDRP and demonstrates that the viral replicase has a dual role in viral RNA replication and infectious particle production, including assembly and release. Lessons from other viruses have proven the importance of functionally and structurally characterizing the viral polymerases to develop direct antivirals. In the case of HEV infection, there is an unmet need, especially in patients with chronic hepatitis E who fail to respond to current treatment. Hence, taking into consideration the selection of viral genomes with improved fitness, e.g., harboring the G1634R variant, during ribavirin treatment and the lack of direct antiviral agents to treat chronic hepatitis E, our findings may contribute to drug design targeting this conserved α-helix of the HEV RDRP thumb subdomain. Such a strategy may allow for interference with both viral RNA replication and production as well as fitness.

CONFLICT OF INTEREST

Nothing to report.

AUTHOR CONTRIBUTIONS

All authors designed research. Noémie Oechslin, Nathalie Da Silva, François-Xavier Cantrelle, Xavier Hanoulle, and Jérôme Gouttenoire performed research. Noémie Oechslin, Nathalie Da Silva, François-Xavier Cantrelle, Xavier Hanoulle, Darius Moradpour, and Jérôme Gouttenoire analyzed data. Noémie Oechslin, Xavier Hanoulle, Darius Moradpour, and Jérôme Gouttenoire wrote the manuscript. All authors reviewed the manuscript.

ORCID

Darius Moradpour https://orcid.org/0000-0003-1977-6792
Jérôme Gouttenoire https://orcid.org/0000-0002-7715-1494

REFERENCES

1. Purdy MA, Harrison TJ, Jameel S, Meng XJ, Okamoto H, Van der Poel WHM, et al. ICTV virus taxonomy profile: hepeviridae. J Gen Virol. 2017;98:2645–6.
2. Rein DB, Stevens GA, Theaker J, Wittenborn JS, Wiersma ST. The global burden of hepatitis E virus genotypes 1 and 2 in 2005. Hepatology. 2012;55:988–97.
3. Hoofnagle JH, Nelson KE, Purcell RH. Hepatitis E. N Engl J Med. 2012;367:1237–44.
4. Kamar N, Izopet J, Pavio N, Aggarwal R, Labrique A, Wedemeyer H, et al. Hepatitis E virus infection. Nat Rev Dis Primers. 2017;3:17086.
5. European Association for the Study of the Liver. EASL Clinical Practice Guidelines on hepatitis E virus infection. J Hepatol. 2018;68:1256–71.
6. Kamar N, Selves J, Mansuy JM, Ouezzani L, Péron JM, Guitard J, et al. Hepatitis E virus and chronic hepatitis in organ-transplant recipients. N Engl J Med. 2008;358:811–7.
7. Debing Y, Moradpour D, Neyts J, Gouttenoire J. Update on hepatitis E virology: implications for clinical practice. J Hepatol. 2016;65:200–12.
8. Gouttenoire J, Pollan A, Abrami L, Oechslin N, Mauron J, Matter M, et al. Palmitoylation mediates membrane association of hepatitis E virus ORF3 protein and is required for infectious particle secretion. PLoS Pathog. 2018;14:e1007471.
9. Nimgaonkar I, Ding Q, Schwartz RE, Ploss A. Hepatitis E virus: advances and challenges. Nat Rev Gastroenterol Hepatol. 2018;15:96–110.
10. Koonin EV, Gorbalenya AE, Purdy MA, Rozanov MN, Reyes GR, Bradley DW. Computer-assisted assignment of functional domains in the nonstructural polyprotein of hepatitis E virus: delineation of an additional group of positive-strand RNA plant and animal viruses. Proc Natl Acad Sci U S A. 1992;89:8259–63.
11. Mahilkar S, Paingankar MS, Lole KS. Hepatitis E virus RNA-dependent RNA polymerase: RNA template specificities, recruitment and synthesis. J Gen Virol. 2016;97:2231–42.
12. Jia H, Gong P. A structure-function diversity survey of the RNA-dependent RNA polymerases from the positive-strand RNA viruses. Front Microbiol. 2019;10:1945.
13. Debing Y, Gisa A, Dallmeier K, Pischke S, Bremer B, Manns M, et al. A mutation in the hepatitis E virus RNA polymerase promotes its replication and associates with ribavirin treatment failure in organ transplant recipients. Gastroenterology. 2014;147:1008–11.e7.
14. Todt D, Gisa A, Radonic A, Nitsche A, Behrendt P, Suneetha PV, et al. In vivo evidence for ribavirin-induced mutagenesis of the hepatitis E virus genome. Gut. 2016;65:1733–43.
15. Todt D, Friesland M, Moeller N, Praditya D, Kinast V, Brüggemann Y, et al. Robust hepatitis E virus infection and transcriptional response in human hepatocytes. Proc Natl Acad Sci U S A. 2020;117:1731–41.
16. Wolf YI, Kazlauskas D, Iranzo J, Lucia-Sanz A, Kuhn JH, Krupovic M, et al. Origins and evolution of the global RNA virome. mBio. 2018;9:e02329-18.
17. Szkolnicka D, Pollan A, Da Silva N, Oechslin N, Gouttenoire J, Moradpour D. Recombinant hepatitis E viruses harboring tags in the ORF1 protein. J Virol. 2019;93:e00459-19.
18. Ferrero D, Ferrer-Orta C, Verdaguer N. Viral RNA-dependent RNA polymerases: a structural overview. Subcell Biochem. 2018;88:39–71.
19. Proudfoot A, Hyrina A, Holdorf M, Frank AO, Bussiere D. First crystal structure of a nonstructural hepatitis E viral protein identifies a putative novel zinc-binding protein. J Virol. 2019;93:e00170-19.
20. Frolov I, Agapov E, Hoffman TA Jr, Prágai BM, Lippa M, Schlesinger S, et al. Selection of RNA replicons capable of persistent noncytopathic replication in mammalian cells. J Virol. 1999;73:3854–65.
21. Kummerer BM. Establishment and application of flavivirus replicons. Adv Exp Med Biol. 2018;1062:165–73.
22. Dill V, Eschbaumer M. Cell culture propagation of foot-and-mouth disease virus: adaptive amino acid substitutions in structural proteins and their functional implications. Virus Genes. 2020;56:1–15.
23. Lohmann V, Korner F, Koch J, Herian U, Theilmann L, Bartenschlager R. Replication of subgenomic hepatitis C virus RNAs in a hepatoma cell line. Science. 1999;285:110–3.
24. Blight KJ, Kolykhalov AA, Rice CM. Efficient initiation of HCV RNA replication in cell culture. Science. 2000;290:1972–4.
25. Yi M, Ma Y, Yates J, Lemon SM. Compensatory mutations in E1, p7, NS2, and NS3 enhance yields of cell culture-infectious intergenotypic chimeric hepatitis C virus. J Virol. 2007;81:629–38.
26. Gao M, Nettles RE, Belema M, Snyder LB, Nguyen VN, Fridell RA, et al. Chemical genetics strategy identifies an HCV NS5A inhibitor with a potent clinical effect. Nature. 2010;465:96–100.
27. Spagnolo JF, Rossignol E, Bullitt E, Kirkegaard K. Enzymatic and nonenzymatic functions of viral RNA-dependent RNA polymerases within oligomeric arrays. RNA. 2010;16:382–93.
28. Murray CL, Jones CT, Rice CM. Architects of assembly: roles of Flaviviridae non-structural proteins in virion morphogenesis. Nat Rev Microbiol. 2008;6:699–708.
29. Lindenbach BD, Rice CM. The ins and outs of hepatitis C virus entry and assembly. Nat Rev Microbiol. 2013;11:688–700.
30. Aligeti M, Roder A, Horner SM. Cooperation between the hepatitis C virus p7 and NS5B proteins enhances virion infectivity. J Virol. 2015;89:11523–33.

31. Todt D, Meister TL, Steinmann E. Hepatitis E virus treatment and ribavirin therapy: viral mechanisms of nonresponse. Curr Opin Virol. 2018;32:80–7.

32. Debing Y, Emerson SU, Wang Y, Pan Q, Balzarini J, Dallmeier K, et al. Ribavirin inhibits in vitro hepatitis E virus replication through depletion of cellular GTP pools and is moderately synergistic with alpha interferon. Antimicrob Agents Chemother. 2014;58:267–73.

33. Wimley WC, White SH. Experimentally determined hydrophobicity scale for proteins at membrane interfaces. Nat Struct Biol. 1996;3:842–8.

34. Gautier R, Douguet D, Antonny B, Drin G. HELIQUEST: a web server to screen sequences with specific alpha-helical properties. Bioinformatics. 2008;24:2101–2.

35. Zamyatkin DF, Parra F, Alonso JM, Harki DA, Peterson BR, Grochulski P, et al. Structural insights into mechanisms of catalysis and inhibition in Norwalk virus polymerase. J Biol Chem. 2008;283:7705–12.

SUPPORTING INFORMATION

Additional supporting information may be found in the online version of the article at the publisher's website.
Supplementary Material